5-2014

Alendronate Alters Single Cell Gene Expression of Cortical Osteoblast Lineage Cells During Bone Loss

Ryan Jakob Murphy
Dominican University of California

https://doi.org/10.33015/dominican.edu/2014.bio.05

Alendronate alters single cell gene expression of cortical osteoblast lineage cells during bone loss.

A thesis submitted to the faculty of Dominican University of California

& the Buck Institute of Aging

In partial fulfillment of requirements

for the degree

Master of Science

In

Biology

By

Ryan Murphy

San Rafael, California

May, 2014

CERTIFICATION OF APPROVAL

This thesis, written under the direction of Simon Melov and approved by Mary Sevigny, has been presented and accepted by the faculty for partial fulfillment of the requirements for the degree of Master of Science in Biology. The content and research methodologies presented in this work represent the work of the candidate alone.

Ryan Jakob Murphy, Candidate Date 5/14/2014

Dr. Mary Sevigny, Graduate Program Director Date 5/14/2014

Dr. Simon Melov, Graduate Research Advisor Date 5/14/2014

Dr. Dorn Carranza, Secondary Thesis Advisor Date 5/14/2014

Abstract-

The mineralized matrix of bone makes it difficult to examine specific populations of cells which are integral to the tissue using traditional molecular methods. For this study we examined single cell cortical osteoblasts derived from the femurs of C57BL/6J mice. After isolating single cells from bone, we were able to individually analyze their gene expression profiles using the quantitative polymerase chain reaction (qPCR). The mice used for the study were divided into 4 treatment groups, including ovariectomized mice (OVX) and sham surgical controls (SHAM), treated with or without the anti-resorptive bisphosphonate drug Alendronate, an effective FDA approved therapeutic for slowing bone loss in association with osteoporosis. To administer Alendronate, mice were treated with 100 µg/kg Alendronate weekly via intraperitoneal (IP) injections. After a 16-week period post-surgery, mice were euthanized and bone tissue, including spines and femurs, were preserved for analysis (n= 10 mice per treatment per time point). Single cell cortical osteoblasts were obtained from preserved femur through serial collagenase digestion. Osteoblasts cells were collected by selecting for $CD31^-/CD45^-$/Alkaline $Phosphatase^+$ using fluorescence-activated cell sorting (FACS). Over 100 osteoblast cells per treatment group were analyzed using qPCR for the detection of 96 specific transcripts. We confirmed the effects of bone loss in the mice due to OVX surgery via CT scans of the collected spines and femurs at a resolution of 9µm. We identified unique expression patterns in each treatment subset of osteoblast cells. The single cell gene expression analysis revealed that the cell populations that were undergoing bone loss had genetic signatures with distinctive gene expression profiles. Analysis of cells at

a single cell level may lead to a better understanding of the effects of anti-resorptive agents on the cell populations found within bone.

List of Figures

List of Abbreviations

AAALAC: Association for Assessment and Accreditation of Laboratory Animal Care

ALD: Alendronate

AP: Alkaline phosphatase

Axl4: Homeobox Protein Aristaless-Like 4

BMP7: Bone Morphogenetic Protein 7

BMU: Basic multicellular unit

BV/TV: Bone volume / tissue volume

CD31: Cluster of differentiation 31 / Platelet endothelial cell adhesion molecule

CD45: Cluster of differentiation 45 / Protein tyrosine phosphatase, receptor type, C

COL1A1: Collagen Alpha 1 Chain Type I

CT: Computed tomography

FACS: Fluorescence-activated cell sorting

IACUC: Institutional Animal Care and Use Committees

IGF-1: Insulin-like growth factor 1

IP: Intraperitoneal injection

O: OVX

OA: OVX+Alendronate

OVX: Ovariectomized

RAB15: Ras-Related Protein Rab-15

S: SHAM

SA: SHAM+Alendronate

SHAM: Sham surgery/placebo surgery

SORT1: Sortilin 1

Tr.: Trabecular

qPCR: Quantitative polymerase chain reaction

Table of Contents:

Introduction

Goal of Project:

The main goal of this project is to analyze single cell gene expression profiles in individual osteoblast cells isolated from the bones of ovariectomized mice treated with and without Alendronate treatment, and to identify the changes within the osteoblast expression profiles. The first objective of this experiment is to determine the differences in gene expression between osteoblasts isolated from ovariectomized versus sham treated control mice, and then relate this to bone micro-architecture as determined by micro computerized tomography (umCT). The second objective is to test the differential gene expression profiles from Alendronate treated OVX mice versus OVX controls. These results will help demonstrate how estrogen deficiency and the prevention of bone loss with anti-resoprtives specifically alter the gene expression profiles of primary cortical osteoblasts at the single cell level.

Background:

Bone remodeling is the process in which bone is continuously replaced by new tissue, often in response to fractures or micro damage that occur normally in order to repair damaged bone. It is involved in the maintenance of systemic calcium homeostasis, replacing damaged bone, and controlling the growth and development of bone(*1*). Remodeling occurs due to mechanical stress, hormonal changes and in order to maintain the bone mineral homeostasis. Bone remodeling displays three distinct stages of skeletal growth in humans(*2*). During childhood bone remodeling leads to

skeletal growth that reaches homeostasis at adulthood and with increased age leads to a net loss of bone. Bone itself consists of an extracellular mineralized matrix, collagen and cells. Bone remodeling is modulated by two important cell populations, osteoclasts and osteoblasts(*3*). Osteoclasts are large, multinucleate cells that have abundant Golgi complexes and lysosomal enzymes. They are responsible for bone resorption on the surface of cells through the creation of resorption pits (also known as basic multicellular units, or BMUs). Osteoclasts resorb bone through the processes of acidification and proteolysis of the mineralized matrix. The other cell type, osteoblasts, are responsible for the formation of new bone matrix in the resorption pits created by osteoclasts. Osteoblasts cell are derived from multipotent mesenchymal stem cells which have the potential to differentiate into several cell types including adipocytes, fibroblasts and osteoblasts. Collagen I, the main structural protein within bone, is one of the first proteins synthesized by osteoblasts during bone formation, followed by several non-structural proteins. Osteoblasts complete bone formation by the mineralization of the matrix of the bone. About 15% of mature osteoblasts are eventually embedded into the bone matrix, some of which progress in differentiation to become osteocytes. Osteocytes are cells within the bone that are responsible for mechano-transduction, and modulate the activity of osteoblasts and osteoclasts. The two main types of bone found within the skeleton are known as cortical and trabecular bone. Cortical bone supports the body, protects the organs and is very dense. Cortical bone forms the outer shell of bone and makes up the majority of weight in the human skeleton. Trabecular bone, also known as spongy bone, has a high surface area and contains red bone marrow. Its large surface area facilitates metabolic activity and production of blood cells.

Most major bone related diseases, such as osteoporosis and Paget's disease, occur when there is an imbalance in bone homeostasis due to different rates of bone formation and resorption. Osteoporosis, an age related disease, leads to a lowered bone mineral density that causes an increased risk of bone fracture. Fractures due to osteoporosis usually occur within the hip, ribs, vertebrae and wrist and can often leave the patient bed ridden. Diagnosing osteoporosis can be very difficult because those affected by the disease are largely symptom free until a bone fracture occurs. Osteoporosis predominantly affects women, with roughly 1 in 4 women over the age of 50 affected by the disease while only about 1 in 8 men over the age of 50 develop osteoporosis. There are several causes suspected for the dramatic breakdown of bone homeostasis including impaired osteoblast function, estrogen deficiency, poor vitamin D metabolism, and other conditions including cancer, chronic renal failure and poor nutrition. Glucocoricoid medications, drugs that are used for the treatment of arthritis and other health issues, can weaken bones and lead to osteoporosis. Osteoblast function becomes impaired during aging because of lowered proliferation rates, a shorter functional lifespan, and increased adipocyte formation(*4*). The overall cause of which is currently unknown but leads to weakened bone microarchitecture. One of the most readily identifiable factors modulating osteoporosis in women is the loss of estrogen, due to the effects of menopause. Menopause is the primary reason that osteoporosis occurs at much higher rates in women than men. This can cause osteoclasts, the cells responsible for bone resorption, to be more active and have a longer lifespan(*5*). Estrogen deficiency is also known to increase the activation of BMUs leading to higher rates of bone resorption, and a reduction in osteoclast apoptosis while

at the same time increasing osteoblast apoptosis. These factors lead to high rates of bone resorption that osteoblasts are not able to compensate for with increased age. There are several FDA approved medications for treatment of osteoporosis that combat the disease in different ways that include inhibiting osteoclasts, mimicking estrogen activity and stimulating new bone formation.

Bisphosphonates are a class of drugs that are prescribed for treatment of bone diseases such as Paget's disease, hypercalcemia of malignancy and osteoporosis as they are known to prevent the loss of bone mass. They are named after the two phosphonate (PO_3) groups that are bound to a carbon in their molecular structure. Bisphosphonates have preferential binding to calcium due to the phosphonate groups in their structure. Since bone has a high concentration of calcium, high levels of bisphosphonates accumulate within the bone. When the osteoclasts break down bone they absorb high quantities of the bisphosphonate. The drug then works by inhibiting osteoclasts through apoptosis without affecting the mineralization of new bone(*6*). This leads to a reduction of active osteoclasts cells which then slows the rate of bone breakdown. Bisphosphonates can inhibit the resorption of bone caused by other agents such as vitamin D deficiency, retinoids and calcitrol(7). Bisphosphonate treatment can be more effective in preventing fractures when vitamin D is given in combination. Other drugs that are prescribed that are effective in preventing bone loss and fractures, include Teriparatide and Denosumab, with treatment usually proscribed by balancing the benefits versus potential harm and cost of the drugs(*8*). Bisphosphonates typically have a safe drug profile as they are known to be remarkably selective for their target. There are some mild side effects such as rash, muscle and joint pain and inflammation

of the eye. However this class of drugs is also known to be potentially toxic to the kidney in larger doses, and is associated with a low frequency of osteonecrosis. Bisphosphonate-associated osteonecrosis can cause the death of bone tissue within the jaw. Currently there are about 11 different bisphosphonates used for clinical treatment. Alendronate, known commercially as Fosamax, was one of the first bisphosphonates developed and prescribed to treat osteoporosis and is still currently in use(*9*). Alendronate is not only prescribed for postmenopausal osteoporosis but also for glucocorticoids-induced osteoporosis and male osteoporosis*(10).*

Unlike humans, female mice do not undergo menopause, although they do become infertile at around 11 to 16 months of age. The OVX mouse serves as a model for accelerated bone loss of trabecular and cortical bone because it mimics the effects of menopause from estrogen deficiency(*11*). The OVX mouse loses bone via estrogen deprivation due to surgical removal of the ovaries(*12,13*). This makes the OVX mouse an effective model for mimicking osteoporosis in humans due to menopause. The rate of normal age-related bone loss has been shown to be well defined and consistent within a number of inbred mouse strains which makes it possible to distinguish between bone loss due to normal aging and bone loss due to estrogen deficiency(*14*). C57BL/6J mice normally start losing trabecular bone as early as 6 weeks of age, and this continues up until 24 months of age, while cortical bone mass peaks at around 6 months of age before it starts to decline(*2*). The ovariectomy surgery is known to have a strong effect on both the trabecular and cortical bone health of the C57Bl/6J mouse*(12)*.

MicroCT, or x-ray imaging in 3D at a high resolution, can be used to evaluate the micro-architecture of both cortical and trabecular bone. CT scans can be performed *in*

vivo at a low resolution or *ex vivo* using collected tissues at a high resolution resulting in a more detailed and precise quantification of bone metrics. CT scans are one of the more effective ways of diagnosing osteoporosis because it can be used to determine various bone health metrics for both cortical and trabecular bone non-invasively. These metrics include, but are not limited to, bone volume versus tissue volume, trabecular separation and cortical thickness.

Gene expression analysis is an important tool in biology that is typically performed on homogenates of cells(*15*). Gene expression is usually measured by performing techniques such as quantitative PCR, which has high reproducibility and a wide dynamic range. QPCR, or real-time PCR, is used to amplify and quantify specific DNA targets. One potential problem when using a general homogenate of cells for gene expression experiments is that one cannot distinguish the distribution of targeted transcripts amongst the cell population. It is possible for a detected transcript in a homogenized cell preparation to be evenly distributed within the cells or highly concentrated within a small percentage of the overall cell population. This would mean that the average expression levels detected would not necessarily reflect a typical individual cell in the population. Single cell gene expression allows for the analysis of specific cell types within a population(*16,17*). Single cell analysis is a growing area of transcriptomic research with the potential to uncover new insights within proteomic, transcriptional and metabolic functions of individual cells(*18*). Bengtsson et al.(*19*) previously reported that mammalian cell populations have a lognormal expression pattern. This means that when a cell population is lognormally distributed the average expression level won't reflect the expression levels of a typical cell in the population

because the average expression is potentially based upon a small population of cells with high transcription levels. Using whole homogenates for gene expression analysis also ignores the individual contribution of different cell types. Recent research has identified functionally distinct sub-populations within the osteoblast lineage, further showing the importance of deriving single cells for expression analysis (*20*). Fluorescent activated cell sorting (FACS) is a methodology for sorting cells based on the light scattering of fluorescently labeled cells. FACS can be used as an effective single cell sorting technique(*21)*. This is accomplished by labeling proteins with a fluorophore-conjugated antibody that is only found within the desired cell population(*14, 22*). Single cell analysis can use cells isolated directly from the source, which avoids potential problems of using cells grown *in vitro* that may include potential differences in cell behavior, specific location and physiological state of the cells(*23*).

Summary:

The human skeleton is a complex organ incorporating functions that include blood cell production, supporting the body, calcium storage and endocrine regulation. Osteoporosis is a serious age-related disease that affects a large population, with an estimated 2 million fractures a year, and whose health effects have an annual impact of around $17 billion a year in the United States(*24,25*). Osteoporosis causes low bone mineral density and weakened bone architecture, and leads to an increased risk of bone fractures that at a later ages leads to high mortality rates. In recent years, there have been several breakthroughs in treating age-related bone disorders such as

osteoporosis. This progress has been in part accomplished with the creation of successful animal models that mimic age-related bone loss. A well-accepted animal model of bone loss is the ovariectomized (OVX) mouse. Currently, many studies examining bone and the mechanisms of bone loss use cell culture models, or employ total bone cell homogenates(*26,27*). This method of study is often used because of the difficulty of studying bone cells due to the fact that they are usually encased within an ossified matrix. Using cell cultures is not ideal because it is not well understood how osteoblasts transcriptionally vary from one type of bone to another(*28*). It can also be argued that this approach is suboptimal with regards to appreciating the potential importance of physiological or genetic changes in key cell types within the bone. The Melov laboratory has developed a methodology for isolating osteoblasts (the cell type responsible for bone formation) from intact bone(*16*). Such an approach allows the gene expression of the isolated single cells to be studied one at a time. Single cell analysis does not assume that individual cells within a population have the same gene expression profile, and has powerful advantages over alternative methods that require homogenizing all cells together (including different cell types).

This study analyses the gene expression profile of osteoblasts obtained from bone from the OVX mouse model, with and without bisphosphonate treatment and then identifying the gene expression signatures. Using the established technique, osteoblasts cells were isolated from digested bone, stained with osteoblast markers (CD31-/CD45-/AP+), and then collected using FACS. The isolated osteoblasts were then assayed using qPCR for a set of 96 bone specific genes found within osteoblast populations. This set of specific genes was refined through several control qPCR runs

of osteoblasts obtained from C57/BL6J mice. These optimizing qPCR runs were used in order to eliminate any genes that showed no gene expression in the control osteoblasts. We supplemented new genes using current literature in the field of bone and osteoblast research(*29-31*). These genes included, but were not limited to, sclerostin, an indirect inhibitor of bone formation, AEbp1, a gene that plays a role in adipogenesis and has been found in osteoblasts, and Sox2.

This study will provide the first single cell osteoblast transcriptional profile derived *in vivo* from the OVX mouse model. This paradigm is used to assess the *in vivo* skeletal phenotypes and subsequently relate them to the gene expression changes in freshly isolated cells from the bones of treated versus non treated animals. This study will also show the effects of bisphosphonate (Alendronate) treatment within the transcription profiles of single cells during bone loss due to estrogen loss.

Materials and Methods

Animal Models and Treatment

The mice used in this study were obtained as a single cohort from Charles River Laboratories. The mice had OVX or SHAM surgeries performed on them at 2 months of age by the vendor, and after sufficient recovery time, the mice were shipped to our facility. On arrival the mice were tattooed with a number (1-40) on their tail to aid in identification. The mice were monitored for their health status throughout the study, and weighed every week for a 16-week period. The weights of the individual mice were used to determine the amount of Alendronate administered, and to record the expected weight gain due to estrogen deficiency. Mice that were on bisphosphonate treatment

were given a weekly I.P. injection of 100 µg/kg of Sodium Alendronate (Sigma Aldrich). After 16 weeks of treatment, the mice were euthanized and tissues were collected for analysis. During the euthanasia, all of the mice were visually inspected for the success of the OVX or sham surgery. This was done by looking for the characteristic atrophy normally found within the uterine horns of OVX mice. All animal procedures conformed to Buck Institute IACUC guidelines and AAALAC standard operating procedures

MicroCT Analysis

All of the mice were scanned by µCT *in vivo* at a 35 µm resolution at arrival and a week before they were euthanized. When euthanized, at the end of their treatment, tissues were harvested from the entire cohort of mice in order to preform *ex vivo* scans. The lumbar of the spine and half of the right femurs from each treatment group were collected and preserved in 10% neutral buffered formalin. Both of these tissues were scanned at a 9µm resolution, which allowed for more detailed measurements than that of the *in vivo* (35µm) scans. The raw CT data was further processed in order to create a 3D volume for analysis with Nrecon v1.6 (Bucker, Inc.) using consistent dynamic range values (minimum value: -0.002, maximum value: 0.135) in order to minimize the background noise, ensure detection, and obtain consistent values between each sample. Analysis of the CT data for bone metrics was quantified using image analysis software CtAn v1.13 (Bruker Inc.). The femurs were evaluated for cortical bone at the midshaft and trabecular bone in the growth plate. The midshaft analysis was performed on a 2mm section of femur midsection. The growth plate analysis was performed on a 900 µm region of trabecular bone starting at 600 µm distal from a fixed anatomical

landmark at the start of the growth plate. The spines were evaluated for trabecular bone within the 1st lumbar vertebra. Cortical bone was evaluated using global thresh-holding values of (low) 85 to (high) 255 grey scale values. All of the trabecular bone was thresholded using grey scale values of (low) 60 and (high) 120 in order to avoid detecting more dense cortical bone, and only analyze trabecular bone. Cortical and trabecular bone were quantified using the 2D and 3D analysis packages of CtAn, respectively. The trabecular bone health metrics that were examined include bone volume versus tissue volume, trabecular number (Tr. number), and trabecular separation (Tr. separation). Bone volume versus tissue volume simply measures the total volume of bone versus the total volume of empty space/tissue of the VOI. Tr. number, also known as the structure linear density, enumerates the number of traversals across a solid structure made on a linear path through the trabecular bone region. Tr. separation is the thickness of the empty spaces within the VOI. For cortical bone analysis we looked at bone volume versus tissue volume, crossectional thickness, and area. BV/TV operates under the same principle as defined for trabecular bone analysis. Crossectional thickness and area, look at the thickness and the area of the midshaft donut that makes up the volume of interest.

Single Cell Collection and Analysis

After the mice were euthanized, the isolated femurs were cleaned, and epiphyses from both ends were removed, and the resultant diaphysis was subsequently flushed with PBS in order to remove the majority of marrow and hematopoietic cells

from the femur. Once the femurs had been cleaned they were then preserved in a modified media and stored at -80° C as described in Flynn et al(*16*). In order to obtain the single cell cortical osteoblasts, femurs underwent a series of enzymatic digestions using 0.2% collagenase in a phosphate buffered solution. The collagenase bone digestions occurred within a shaker kept at 37° C for a 30 minute period. Before the second collagenase digestion, the femur was finely crushed in order to increase the yield of osteoblast lineage cells by dispersing the bone cells. After the collagenase digestions, the disrupted bone was spun down and the supernatant was removed. The supernatant was then spun down in order to obtain the pellet of cells to be sorted. A mild fixative was added to the cell pellet in order to better preserve RNA integrity. At this stage of single cell isolation there was a heterogeneous cell population from the bone matrix which was then stained using antibodies against specific cellular markers (CD31-/CD45-/AP+). The CD31 marker is found in osteoclast cells and CD45 is found in hematopoietic cells, while alkaline phosphatase is specific for the osteoblast lineage as it is involved in laying down bone. Using florescent-activated cell sorting (FACS) we selected for cells that were detected with negative CD31, CD45 and positive for AP florescence. A minimum of four individual biological replicates were used per treatment group for FACS and to isolate the individual cells. The osteoblast single cells were collected via micro-pipet and transferred to individual tubes for gene expression analysis. At least 110 individual osteoblast cells were collected for each treatment group with an overall total of 480 individual osteoblast lineage cells collected. These processed cells were then frozen at -80℃ until qPCR gene expression analysis.

Single Cell Gene Expression

The isolated individual osteoblasts cells were assayed using a single cell qPCR procedure. The procedure uses direct reverse transcription and specific target amplification prior to microfluidic qPCR. The individual cells were isolated using a micro-manipulator and then placed in PCR tubes with a small volume of 1-2 µl that were then immediately frozen on dry ice and then stored at -80° C. When the qPCR was ready to be performed the cells were thawed on ice. Then the cells were pre-amplified using specific target amplification of relevant genes containing all 96 assay primers sets for 18 cycles using the Cell-Direct RT-qPCR kit (Invitrogen). The single cell pre-amplified product was then diluted 1:5 in a DNA suspension buffer and then assayed using Fluidigm's 96.96 nanofluidic qPCR on a Biomark HD system. Biotium's EvaGreen DNA binding dye was used to detect amplified product according to Fluidigm's advanced development protocol #30(*23*). The exported qPCR data files were then normalized using Singular R analysis package (v1, Fluidigm) in order to obtain Log2Expression values for each reaction.

Statistical analysis

All of the statistical comparisons for this study were tested using a non-parametric randomization test using the statistical software R (*16*). Treatment groups were compared and the null was rejected if $p<0.05$. These statistical tests were performed in order to avoid the assumption of a normal distribution within our samples, especially for the single cell gene expression analysis. Pairwise comparisons were made using permutation test and multiple testing correction was applied to identify

differential gene expression (Benjamini-Hochberg. 5% FDR). The CT statistical analysis was performed by comparing the statistical differences between the specific treatment groups including: SHAM versus OVX, SHAM versus OVX+ALD, SHAM versus SHAM+ALD and OVX versus OVX+ALD. ANOVA P-value testing was used to determine the statistical differences in gene expression for each treatment group.

Results

In order to derive a source for our osteoblast lineage cells we obtained a cohort of 40, 2-month old C57BL/6J mice. Half of the mice had OVX surgery performed while the other half had a SHAM surgery. Once at our facility the mice were divided into four groups of 10, with one group from each surgical treatment receiving Alendronate (100 µg/kg) treatment once every week via I.P. injection. This resulted in 4 treatment groups: OVX, OVX+ALD, SHAM and SHAM+ALD. After a 16 week period, the mice were euthanized and tissues were collected for osteoblast cell collection for qPCR and CT scans (Figure 1).

Estrogen Depleted Bone Loss is attenuated or reversed by Alendronate

The weights of the mice were closely monitored in order to determine the success or failure of the OVX surgery(Figure 2), as occasionally the surgical procedure is not successful. The OVX estrogen deficient mice showed the expected weight gain at approximately 59 to 66 days post-surgery when compared to the SHAM controls. This

elevated weight gain was maintained for the full 16 weeks in the OVX group. However by the end of the 16 week treatment, the OVX+ALD weights were not significantly different from the SHAM treatments. There was no statistically significant difference in weights between the SHAM and SHAM+ALD treatment groups throughout the study. After the mice were euthanized for tissue collection their uterine horns were visually inspected for atrophy (Figure 2). All of the OVX treatment mice showed clear atrophy in their uterine horns, as expected, while the SHAM mice had uterine horns that had proper blood flow and normal appearance, confirming that the OVX procedure was successful in the OVX mice used in this study.

In order to show that estrogen deficiency results in bone loss in mice and that treatment with Alendronate can modulate/attenuate these effects, and even lead to greater bone mass, spines and femurs were collected for 3D visualization via CT scans. The first lumber vertebrae (Lumbar 1) of the spine was scanned at a high resolution and subvolumed in order to investigate the bone health metrics of the trabecular bone for each treatment group of mice (n = 9)(Figure 3). The OVX mice showed a significant decrease in Tr. number, along with a significant increase in Tr. separation when compared to the SHAM mice. This indicates that there is ongoing bone loss in the OVX mice as there is not only a clear reduction in bone mass but an increase in the empty spaces within the trabecular bone network. Treatment with Alendronate in the OVX mice was able to reverse the increase in Tr. separation, and lead to higher BV/TV and Tr. number values. SHAM+ALD treatment mice also showed improved bone metrics but only showed enhanced metrics in Tr. separation when compared to the OVX+ALD mice.

The right femurs for 5 mice per treatment group were collected for micro CT while the rest of the femurs were collected for single cell osteoblast collection. Analysis of the bone loss found in the femurs was important to characterize since the osteoblasts cells were derived from the femur. The femurs were scanned at a high resolution (9µm) and subvolumed in order to investigate the cortical bone of the midshaft, and the trabecular bone of the femoral growth plate (Figure 4). The cortical midshaft (mid-point +/- 1mm) of the femur showed a significant reduction in mean crossectional area and thickness of the femur in OVX mice versus the SHAM control mice. There was no difference in the overall bone volume in the OVX mice when compared to the SHAM mice. OVX+ALD did not seem to have a significant impact on the changes in cortical thickness and cortical area observed in the OVX but there was a trend towards an improvement both metrics, almost restoring them to the levels found in the SHAM controls. As expected the SHAM+ALD had the healthiest bone metric values out of all the treatment groups. These results indicate that there is a likely thinning of the cortical bone in the midshaft of the femur that is to be expected from the OVX surgery. This showed that the targeted source of osteoblasts cells, the cortical midshaft of the femur, was clearly undergoing bone loss.

The femurs were also examined for trabecular bone loss in the femoral growth plate. The BV/TV and Tr. number were significantly higher in both of the ALD treatment groups. The Tr. separation was also significantly lower in both the ALD treatment groups when compared to their OVX and SHAM counterparts. There was a significant change in Tr. Separation and Tr. number in the OVX versus SHAM mice along with a small, but significant, difference in BV/TV. This suggests that there is a change in the

femoral bone architecture due to the estrogen deficiency from OVX surgery. Overall the results from the bone analysis of both the femur and the spine demonstrated that the Alendronate treatment is either able to slow or prevent the bone loss that occurs due to estrogen deficiency in the mice, consistent with prior literature.

Single cell gene expression of isolated osteoblast cells

Once it was established that both the ovariectomy procedure and the pharmacological intervention were affecting bone loss as expected we moved on to isolating the single cell osteoblasts from the femurs of the mice using a previously established technique developed by the Melov lab. This method involved using multiple collagenase digestions of the femur in order to obtain the cell population. The cells were then labeled using fluorescent antibodies for CD31, CD45 and Alkaline Posphatase (AP). Once the cells were properly labeled, FACS was used to obtain a pure population of osteoblast cells. At least 4 biological replicates were used for each treatment group with approximately ~120 single cells isolated per group. The collected osteoblast cells were then prepared for single cell gene expression analysis using specific target amplification for 96 gene expression assays (Figure 5). The amplified material was then run on nanofludic qPCR arrays to generate the single cell expression profiles. The qPCR amplification data was analyzed using Fludigm's single cell gene expression package in the R statistical programming environment.

The resulting log2 expression values of each gene were used for statistical analysis, including the generation of a heat map of the gene expression values for each osteoblast (Figure 6). The genes in the heat map were organized using hierarchical

clustering in order to identify groupings of genes that had a similar expression pattern among the four treatment groups. In order to determine whether or not one specific animal affected any of the expression results we labeled each cell with the animal ID. By doing this we were able to determine that none of the osteoblasts derived from a specific animal drove any of the osteoblast expression patterns that were found in the heat map. Along the side of the heat map the individual osteoblast cells were labeled with their specific treatment group and clustered in order to determine if any profiles appeared. In order to effectively identify if there were any novel subsets of osteoblast gene expression principal component analysis was performed on the single cell gene expression data (Figure 7). The PCA analysis was used to reveal if either estrogen depletion or Alendronate treatment affected the overall gene expression profile. The PCA analysis revealed that there was a group of osteoblast cells that did segregate based on O, OA and SA treatment. However, there were no clusters of cells that segregated based on an individual treatment group. This lack of segregation due to treatment is not necessarily surprising as it is likely due to the fact that all of the osteoblasts cells were derived from a purified population assayed for bone specific markers and bone associated genes.

In order to determine if there were significant changes in gene expression within the different single cell osteoblast treatment groups, we assessed the log2 expression values of each gene using ANOVA P-value testing. These results were then graphed using violin plots of the gene expression data for each individual gene, with expression separated based on treatment group (Figure 8). Every extension of the violin plot, on the y axis, represents the expression level of the specific gene, with the cell count

indicated by how wide the violin plot was at different log2 expression values. The violin plots of the genes were organized with genes that had greatest differential expression between treatment groups located at the top of the figure and those with the lowest differential gene expression at the bottom. The violin plots showed that there were a number of genes with differential gene expression within the osteoblast treatment groups.

The largest differential gene expression profiles were found in genes that had higher levels of expression in cells located in the OA, S and SA treatment groups. This indicates that estrogen depletion causes gene alterations that seem to be reversible with Alendronate treatment in many of our selected genes. The functions of these genes ranged from cell cycle control, ossification, cell differentiation, osteoblast cell fate, developmental pathways, to mitochondrial associated genes. The other common expression profile within the genes had higher expression values in cells in the O, OA and SA treatment groups. Many of these genes are mitochondrial related and involved in electron transport, NADH dehydrogenase and even cellular response to oxidative stress. This grouping of genes indicates that there might be a subpopulation of genes in osteoblasts that are more highly expressed due to both estrogen deficiency and Alendronate treatment. The two other notable expression patterns found within violin plots had genes with higher expression values in the SHAM treatment groups, and in both Alendronate treatment groups. The genes with high expression in only the SHAM treatments likely represent genes that are lost due to estrogen deficiency regardless of Alendronate treatment. The function of these genes included osteoblast differentiation, protein transport and mitochondrial related actions. In the same regard the genes with

higher expression values found only in Alendronate treatment groups were likely due to the administration of the drug. Both BMAL1 and CYC1 had higher gene expression values due to Alendronate treatment. The only gene that showed higher expression values, though only slightly, in the OVX treated cells was NOTCH3, which is known to regulate cell fate and impair osteoblast differentiation.

Discussion

Both the ovariectomy mouse model and bisphosphonate treatment have well defined impacts on bone loss. However, these treatments' *in vivo* effects on osteoblast lineage cells are poorly defined. In order to gain a better understanding of how these treatments work within the targeted tissue, we applied a new single cell method to isolate and profile the gene expression of individual osteoblast cells. This study combines both ovariectomized mice and Alendronate treatment to better understand their effects on osteoblasts and osteoblast signaling.

Once the efficacy of the surgery was determined, via tracking of the expected weight gain and visual inspection of atrophy within the uterine horns of the mice, we wanted to confirm the expected bone phenotypes. High-resolution microCT scans of both the spine and femur were used to confirm that estrogen deficiency caused bone loss and that Alendronate treatment could lead to improved bone health. The CT data showed that estrogen deficiency had a significantly negative impact on both trabecular and cortical bone health metrics and that Alendronate treatment was able to slow or reverse much of the bone loss seen in the OVX mice and even improved bone health

metrics in the SHAM control mice. Alendronate treatment was only able to lead to significantly increased cortical bone health in the SHAM mice but a clear trend towards increased bone health was seen in the OVX mice. These microCT results allowed us to confirm that the each treatment group altered bone health metrics as expected.

With the osteoblast lineage cells successfully isolated, qPCR was performed for 96 genes in order to generate gene expression profiles for all of the collected cells. The overall expression of mRNA within these cells was low but measurable when compared to other cell types(*23*). The principal component analysis of the expression data showed that neither the estrogen depletion nor the Alendronate treated cells seemed to segregate based solely on individual treatment group. However when the expression levels for each gene were analyzed many differentially expressed genes were identified. The most common expression profile found within our selected genes had higher levels of expression in the OA, S and SA treatment cells. These genes had significantly lower expression levels in the OVX treated cells and saw restored expression levels in OVX mice that were treated with Alendronate. These results suggest that these genes are responsible for modulating bone loss in this model. This conclusion seems likely as many of the genes found in this expression profile are known to be responsible for bone formation and osteoblast development, such as Axl4, BMP7, IGF1 and Osterix. These expression profiles may account for the poor bone health metrics found in the OVX mice and the improved bone health observed in the OVX+ALD treatment mice. We examined the profiles of genes within this expression profile for any interesting expression changes that could validate the biological changes seen in the bones of the mice used in this study. One gene that stood out was IGF1 which is known to be a key gene in the

signaling pathway of bone development and partially responsible for osteoblast differentiation. For these reasons IGF1has a vital role in terms of the development and function of the skeletal system. This indicates that estrogen deficiency, in part, causes bone loss due to low levels of IGF1 expression and that Alendronate is able to reverse the change in IGF1 expression. Interestingly IFG1-receptor had high expression levels within all of treatment groups, with the lowest levels of expression found in the SHAM treatment cells. This indicates that the levels of IGF1 expression are a key limiting factor in the IGF1 bone formation pathway rather than the amount IGF1-recptor found within the osteoblast cells. CCRN4L, or nocturnin, was another interesting gene that showed high expression levels in OA, S, and SA treated osteoblast cells. This result was unexpected as several studies have found that nocturnin suppresses the I1 anabolic pathway and lowers IGF1 expression. However, nocturnin may have some other beneficial effects on bone health, even with its negative effects on IGF1, as it was highly expressed in OA, S and SA treatment groups, the treatment groups that had best bone health metrics.

The other major expression profile we discovered in our qPCR data had genes with higher expression in all treatment groups except for the SHAM treatment cells. Genes within this expression profile had several different functions but there were many genes, such as ND3, CYTB and ND4L, which had mitochondrial related functions. The increased expression of mitochondrial genes could indicate higher levels of mitochondria, and an increase in energy production in the osteoblast cells which would be expected to improve the rate of bone formation. This would help to explain why the SHAM+ALD mice had improved bone health metrics when compared to the SHAM

mice. Interestingly, these genes were also more highly expressed in the OVX treatment cells but it does not seem like their increased expression is sufficient for bone development.

There were several genes that showed higher expression levels in only the SHAM treatment groups. These genes appear to be unaffected by Alendronate treatment in our osteoblast cells. The genes that had higher expression only in the SHAM osteoblasts have functions that include bone formation, osteoblast differentiation and regulation of calcium ions. COL1A1, Osteopontin, and SORT1 are examples of these genes that are also known to have positive effects on bone health. COL1A1, the gene for Collagen Type I Alpha 1, is one of the major structural components of bone that is laid down by osteoblasts. This makes COL1A1 a interesting target to investigate further in order to help combat bone loss due to estrogen deficiency as Alendronate treatment was not able to reverse its loss in osteoblasts. Notch3 was one of the few genes that was more highly expressed in only the OVX treatment cells. Notch3 is a receptor for membrane bound ligands that has been found in osteoclasts and importantly has been discovered to arrest osteoblast differentiation. Genes like Notch3 and COL1A1, whose expression seems to be unaffected by bisphosphonate treatment, offer up new potential targets for the treatment of osteoporosis and other bone related disease, either in conjunction or separate from Alendronate treatment.

This study measured single cell gene expression of *in vivo* derived osteoblast cells. We were able to identify a suite of differentially expressed genes due to both estrogen depletion and Alendronate treatment, from an otherwise relatively homogenous gene expression profile within the osteoblast cells. This potential to

analyze gene expression changes at the single cell level allows for the testing of other osteoporosis treatments with unknown efficacy in the OVX model along with the ability to analyze single cells within other future model systems.

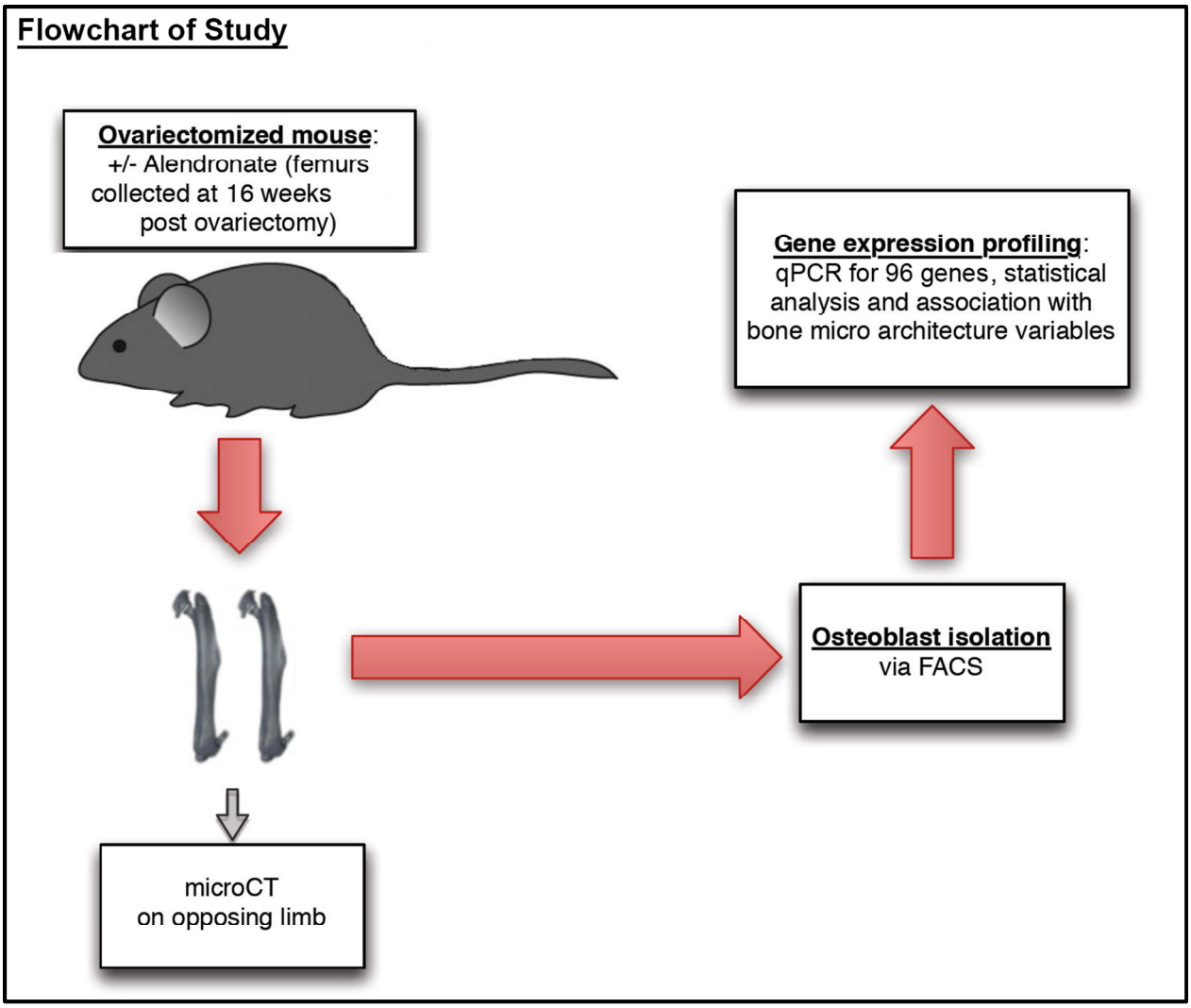

Figure 1. *Flowchart of Study.* Outline of the steps involved in this study. Briefly, 40 C57BL/6 mice were obtained with an ovariectomy surgery performed on half of the cohort and a SHAM surgical control preformed on the other half. The mice were kept for 16 weeks with half of each surgical group on Alendronate treatment. After the 16 week period the mice were euthanized for collection. Femurs were then microCT scanned to evaluate the bone microarchitecture or used for osteoblast isolation. QPCR was then preformed on all obtained osteoblasts.

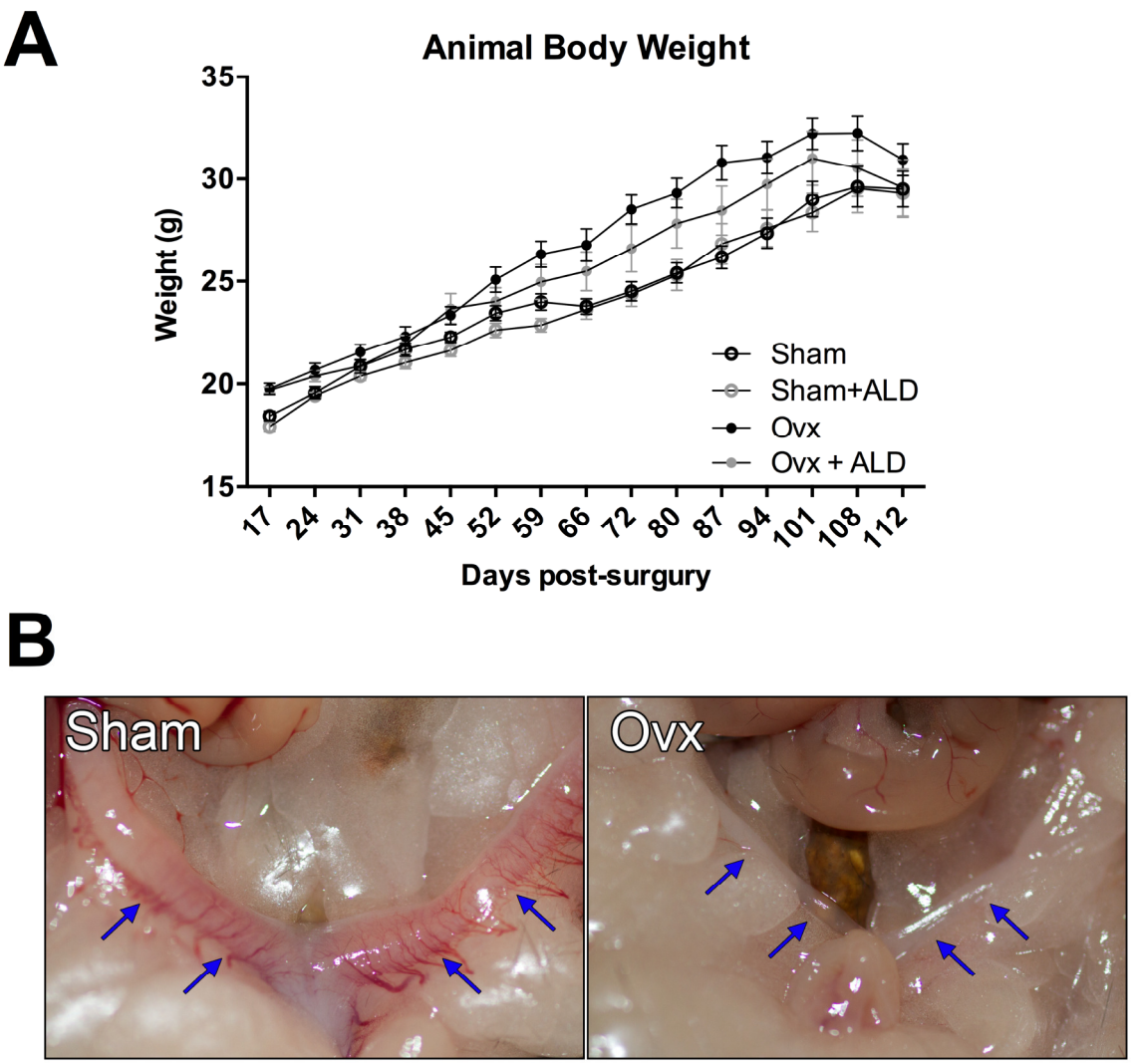

Figure 2. *Efficacy of OVX & SHAM Surgery*. The weights of the mice were tracked weekly at the start of the Alendronate treatment in order to observe the success of the OVX surgery. As expected, the mice with the OVX surgery gained more weight versus the SHAM controls at around 8 weeks post-surgery. The uterine horns of each mouse were examined after euthanasia in order to confirm atrophy of the uterine horns. The SHAM uterine horns had a normal appearance while the OVX uterine horns showed atrophy, as indicated by the blue arrows.

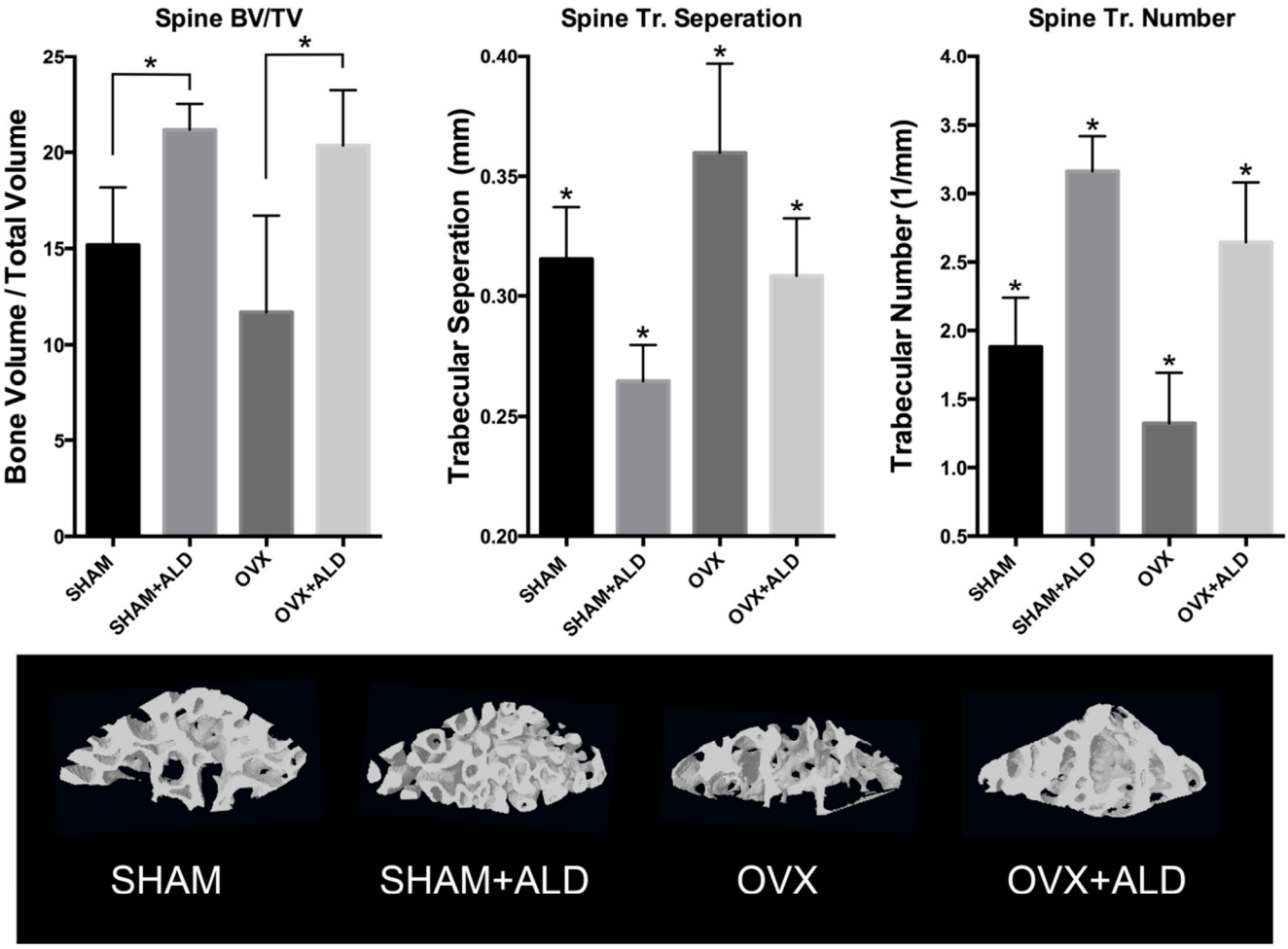

Figure 3. *Ex vivo CT analysis of Spine 16 weeks post-surgery*. Lumbar 1 of all the mice were scanned by µCT, *ex vivo*, at a high resolution (9 um) in order to analyze the effects of estrogen depletion and Alendronate treatment on the trabecular bone health of the mice. The bone health metrics that were used for analysis were BV/TV, Tr. separation and Tr. number (n= 9 per group, $p<0.05$). The estrogen depleted OVX mice showed a significant reduction in BV/TV and Tr. Number and increased Tr. separation. Treatment with alendronate reversed these changes in the trabecular bone and lead to improved trabecular bone health in the SHAM control mice. Below the bar graphs are images of 3D models of the volume of interested analyzed that are representative for each treatment group in the study.

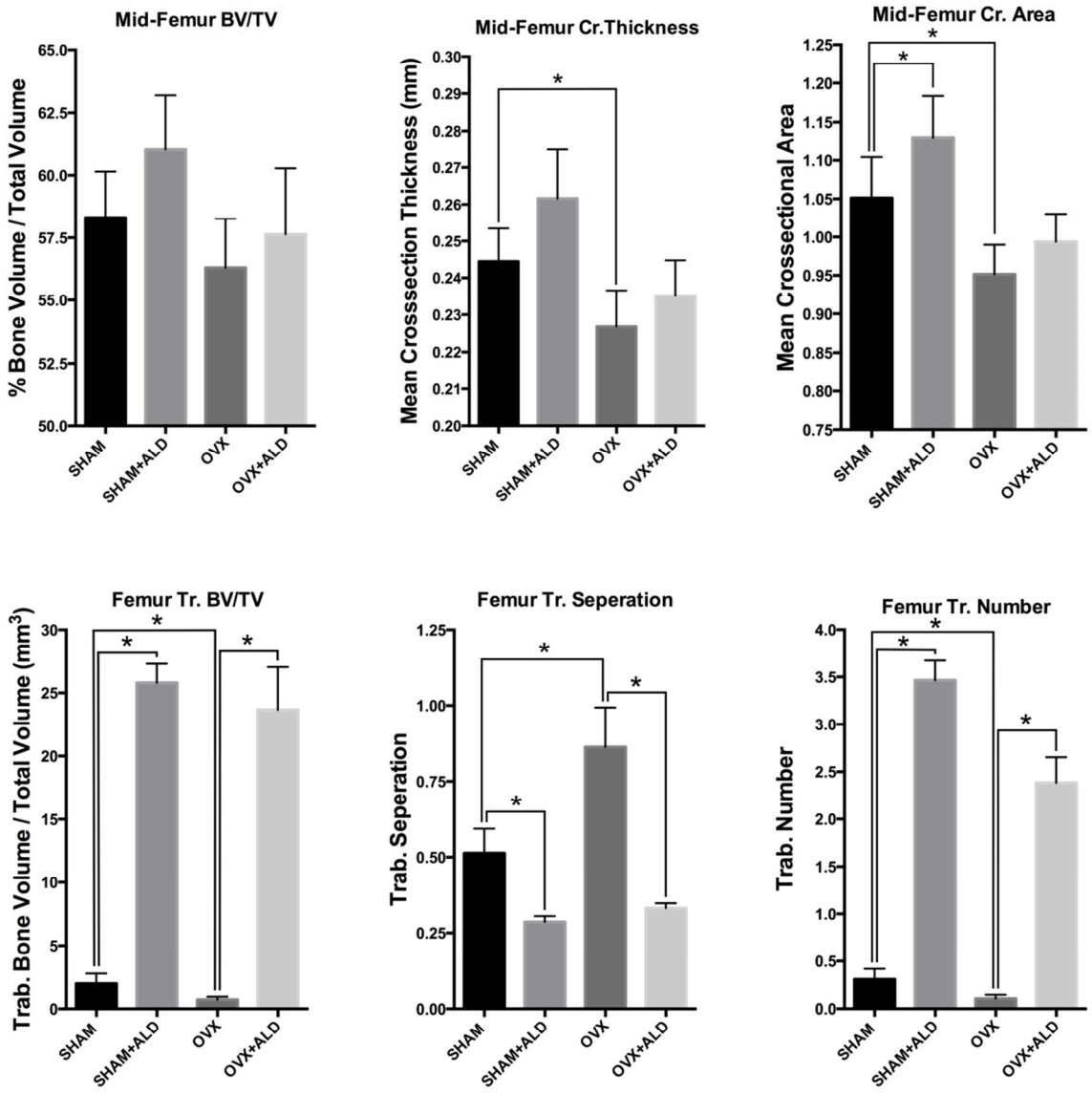

Figure 4. *Ex vivo CT analysis of femurs 16 week post-surgery*. In order to analyze bone loss from the area in which the osteoblast cells were derived femurs (n= 5 per group, $p<0.05$) were collected for each treatment group. The femurs were scanned by µCT, ex vivo, at a high resolution (9um). The cortical bone, the midshaft of the bone, and the trabecular bone, a section of the growth plate, were analyzed using standard bone metrics. The mean crossectional area and thickness of the femur midshaft were significantly reduced in the OVX treatment versus the SHAM control while the overall bone volume showed no significant difference. The trabecular BV/TV, and Tr. Number were both significantly higher, along with a significant decrease in Tr. Separation, in both of the alendronate treatment groups. In the trabecular bone there is significant difference in Tr. separation between OVX and SHAM treatment mice. There is also a small but still significant decrease in BV/TV and Tr. number in the OVX versus SHAM mice. This indicates that there is still a potential change in the bone architecture of the femur due to estrogen deficiency.

Genes used for qPCR Assays							
AEBP1	Axl4	BGLAP	BGN	BMAL1	BMP6	BMP7	BTG2
CCNA2	CCNB1	CCR6	CCRN4L	CD105	CD31	CD44	CD45
CD5	CD79A	CD79B	CDK2	CDKN1B	CHRNA1	CKIP1	COL1A1
COL1A2	COX1	COX2	CRYAB	CTNNB1	CXCL12	CXCR4	CYC1
CYP51	CYTB	EFNB2	EPHB4	FGF21	FOXO1	FOXO3	HLA_DR
ID4	IGF1	IGFBP2	IGFR1	KERA	LEPRINR	LHX2	LIQCR10
LRP130	MGP	MMP13	MMP14	MSX2	ND2	ND3	ND4
ND4L	ND5	ND6	NDUFB2	NDUFS4	NDUFV1	NOTCH3	Notch4
OMD	Osteopontin	Osterix	Pax1	PER1	PER2	PGC1A	PGC1B
Pleiotropin	POSTN	PPARALPHA	RAB15	REV_ERBA	Runx2	Sclerostin	SMAD5
SMURF1	SORT1	SOST	SOX2	SOX9	SPROUTY1	SPROUTY2	TFAM
TNFSF11	TNMD	TRPM8	VCAN	WIF1	WISP1	WNT10B	WNT5A

Figure 5. Table *of 96 genes used for qPCR gene expression assays.* This table shows all 96 bone and osteoblast related genes that were used for the qPCR assays of the single cell isolated osteoblasts obtained in this study. The genes selected were mainly bone specific and bone related genes along with some cell cycle and mitochondrial related genes.

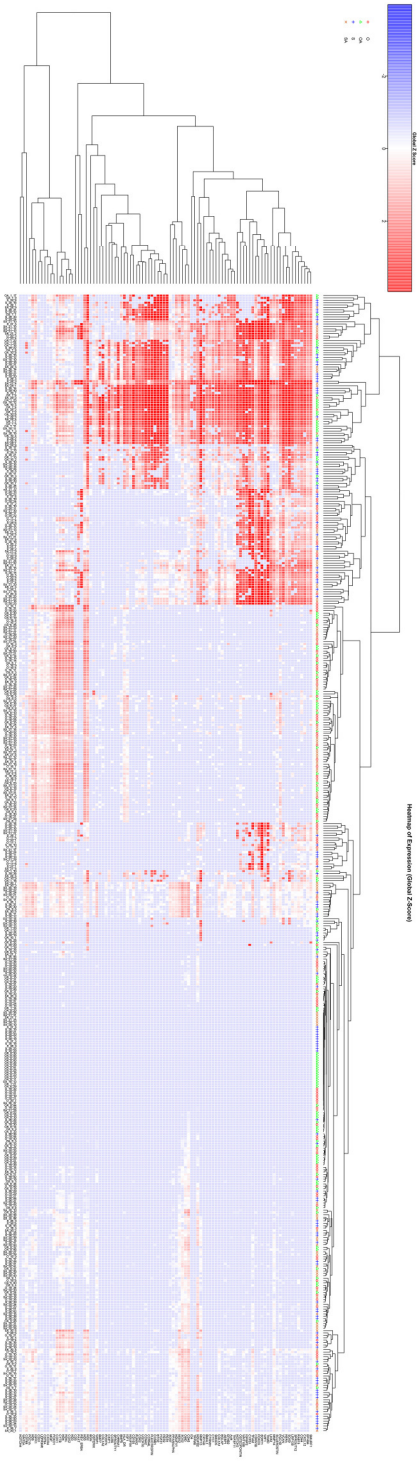

Figure 6. *Heat map of single cell osteoblast gene expression*. The log2 expression values for each cell are shown based on a global z scale score with red indicating a high gene expression value and blue indicating a low expression value. The genes were clustered in order to identify any expression profiles among the 4 treatment groups of osteoblast cells. Along the side of each row of the heat map cells were labeled with their treatment group and the animal ID from which they were originally derived. This was done to determine if any of the expression patterns were due treatment group or the individual mouse they were derived from.

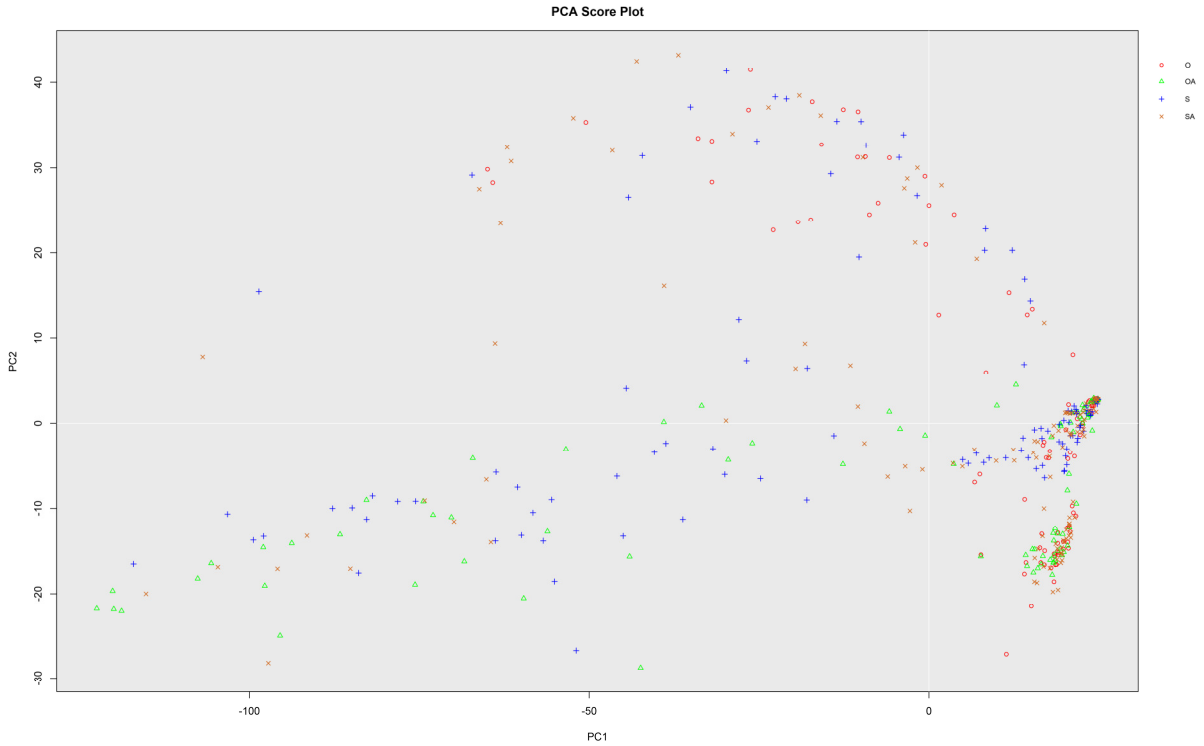

Figure 7. *Principal Component Analysis of single cell gene expression data*. The gene expression profiles of the 480 isolated osteoblasts generated using 96 gene expression assays were examined with Principal Component analysis. The PCA analysis indicates that there are very little distinct profiles observed among the treatment groups. The one unique subset that is found within the cell populations, located in the lower right quadrant of the PCA score plot, shows cells clustering due to O, OA, and SA treatment.

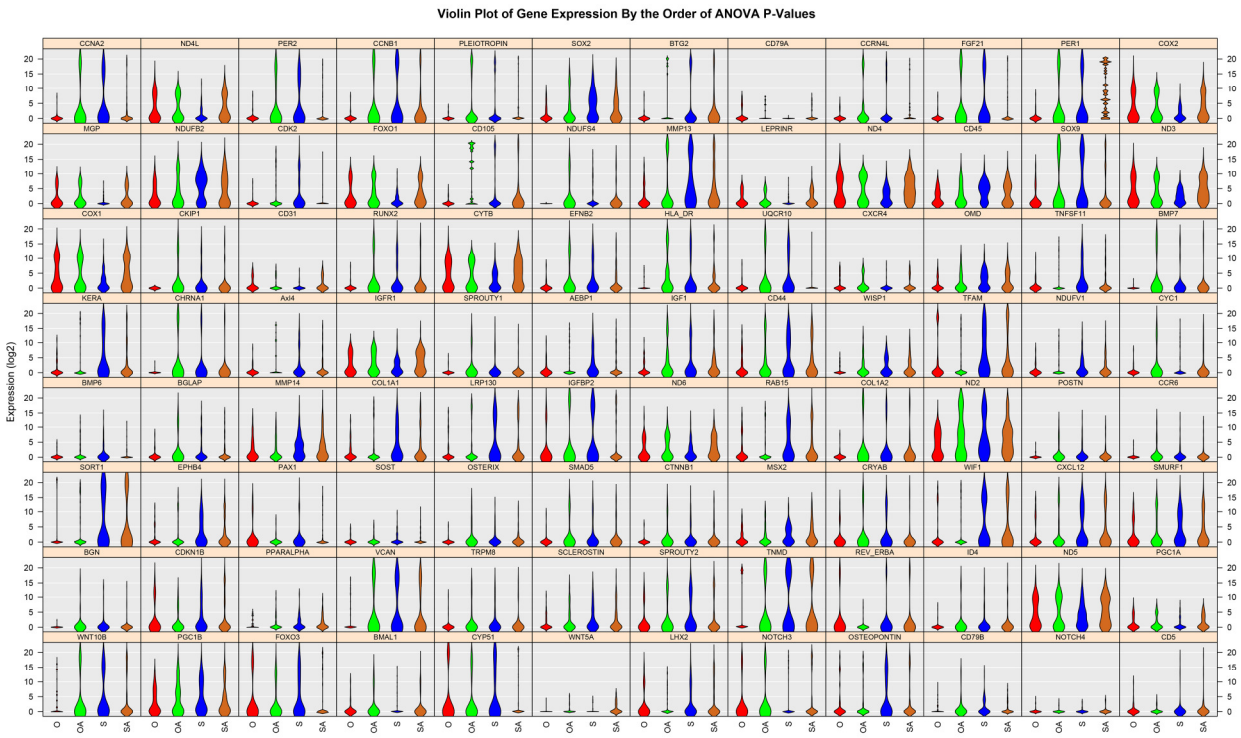

Figure 8. *Violin Plots of the Log2 Gene Expression Levels for each Treatment group.* All expression data from the osteoblast qPCR runs was used to find the Log2 Expression levels for all 96 genes we examined in this study. The Log2 Expression levels were than used to create violin plots for the expression values of all 96 genes for each treatment group (S = SHAM, SA = SHAM + ALD, O = OVX, and OA = OVX + ALD). Genes were organized due to differential expression among the four treatment groups, with those having the greatest differential expression located at the top left of the figure and genes with the lowest differential expression found at the bottom right section of the figure.

—

References

1. A. E. Kearns, D. F. Kallmes, Osteoporosis primer for the vertebroplasty practitioner: expanding the focus beyond needles and cement. *AJNR Am J Neuroradiol* **29**, 1816 (Nov, 2008).
2. F. A. Syed, T. Melim, Rodent models of aging bone: an update. *Curr Osteoporos Rep* **9**, 219 (Dec, 2011).
3. D. J. Hadjidajus and I. I. Androulakis, Bone Remodeling. *Annals of New York Academy of Sciences* **1092**, 385 (Dec, 2006)
4. M. Kassem, P. J. Marie, Senescence-associated intrinsic mechanisms of osteoblast dysfunctions. *Aging Cell* **10**, 191 (Apr, 2011).
5. M. N. Weitzmann, R. Pacifici, Estrogen deficiency and bone loss: an inflammatory tale. *The Journal of clinical investigation* **116**, 1186 (May, 2006).
6. D. G. Hesslein *et al.*, Ebf1-dependent control of the osteoblast and adipocyte lineages. *Bone* **44**, 537 (Apr, 2009).
7. C. J. Rosen, Exploiting new targets for old bones. *J Bone Miner Res* **25**, 934 (May, 2010).
8. M. H. Murad et al., Comparative Effectiveness of Drug Treatments to Prevent Fragility Fractures: A Systematic Review and Network Meta-Analysis. J Clin Endocrinol Metab **97**, 1871 (June 2012).
9. R. G. Russell, Bisphosphonates: the first 40 years. *Bone* **49**, 2 (Jul, 2011).
10. P. J. Prinsloo and D. J. Hosking, Alendronate sodium in the management of osteoporosis. Ther Clin Risk Manag **2**, 235 (Sep 2006).
11. J. Klinck, S. K. Boyd, The magnitude and rate of bone loss in ovariectomized mice differs among inbred strains as determined by longitudinal in vivo micro-computed tomography. *Calcif Tissue Int* **83**, 70 (Jul, 2008).
12. M. L. Bouxsein *et al.*, Ovariectomy-induced bone loss varies among inbred strains of mice. *Journal of bone and mineral research: the official journal of the American Society for Bone and Mineral Research* **20**, 1085 (Jul, 2005).

13. D. Seidlova-Wuttke, B. T. Nguyen, W. Wuttke, Long-term effects of ovariectomy on osteoporosis and obesity in estrogen-receptor-beta-deleted mice. *Comp Med* **62**, 8 (Feb, 2012).
14. P. Le *et al.*, A high-fat diet induces bone loss in mice lacking the Alox5 gene. *Endocrinology* **153**, 6 (Jan, 2012).
15. W. Luo, M. S. Friedman, K. D. Hankenson, P. J. Woolf, Time series gene expression profiling and temporal regulatory pathway analysis of BMP6 induced osteoblast differentiation and mineralization. *BMC Syst Biol* **5**, 82 (May, 2011).
16. J. M. Flynn, S. C. Spusta, C. J. Rosen, S. Melov, Single cell gene expression profiling of cortical osteoblast lineage cells. *Bone* **53**, 174 (Dec, 2012).
17. A. Stahlberg, M. Bengtsson, Single-cell gene expression profiling using reverse transcription quantitative real-time PCR. *Methods* **50**, 282 (Apr, 2010).
18. S. H. Kim, D. Fourmy, T. Fujii, Expanding the horizons for single-cell applications on lab-on-a-chip devices. Methods Mol Biol **853**, 199 (2012).
19. M. Bengtsson, A. Stahlberg, P. Rorsman, M. Kubista, Gene expression profiling in single cells from the pancreatic islets of Langerhans reveals lognormal distribution of mRNA levels. *Genome Res* **15**, 1388 (Oct, 2005).
20. S. C. Rawlinson *et al.*, Adult rat bones maintain distinct regionalized expression of markers associated with their development. *PLoS One* **4**, e8358 (2009).
21. K. D. Miller, N. B. Pefaur, C. L. Baird, Construction and screening of antigen targeted immune yeast surface display antibody libraries. *Curr Protoc Cytom* **Chapter 4**, Unit4 7 (Jul, 2008).
22. C. Esser, C. Gottlinger, J. Kremer, C. Hundeiker, A. Radbruch, Isolation of full-size mRNA from ethanol-fixed cells after cellular immunofluorescence staining and fluorescence-activated cell sorting (FACS). *Cytometry* **21**, 382 (Dec, 1995).
23. J. M. Flynn, L. F. Santana, S. Melov, Single cell transcriptional profiling of adult mouse cardiomyocytes. *J Vis Exp*, e3302 (2011).
24. M. M. Iqbal, Osteoporosis: epidemiology, diagnosis, and treatment. *South Med J* **93**, 2 (Jan, 2000).
25. R. Burge *et al.*, Incidence and economic burden of osteoporosis-related fractures in the United States, 2005-2025. *Journal of bone and mineral research : the*

official journal of the American Society for Bone and Mineral Research **22**, 465 (Mar, 2007).

26. B. Kulterer *et al.*, Gene expression profiling of human mesenchymal stem cells derived from bone marrow during expansion and osteoblast differentiation. *BMC Genomics* **8**, 70 (2007).
27. L. J. Foster , P.A. Zeemann, C. Li, M. Mann, O. N. Jensen, and M. Kassem, Differential expression profiling of membrane proteins by quantitative proteomics in a human mesenchymal stem cell line undergoing osteoblast differentiation. *Stem Cells* **23**, 1367 (Oct, 2005).
28. S. S. Varanasi et al., Skeletal site-related variation in human trabecular bone transcriptome and signaling. *PLoS One* **5**, 5 (Oct, 2010).
29. F. Paic, et al., Identification of Differentially Expressed Genes Between Osteoblasts and Osteocytes. *Bone* **45**, 682 (Oct 2009).
30. P. J. Marie, Signaling Pathways Affecting Skeletal Health. *Curr Osteoporos Rep* **10,** 190 (Sep 2012).
31. S. Marcellini, J. P. Henriquez and A. Bertin, Control of osteogenesis by the canonical Wnt and BMP pathways in vivo. *Bioessays* **34**, 953 (Nov 2012).
32. S. Yakar, H. W, Courtland and D. Clememons, IGF-1 and Bone: New Discoveries From Mouse Models*. J Bone Miner Res* **25**, 2543 (Aug 2010).
33. S. Zanotti and E. Canalis, Notch signaling and bone. *IBMS BoneKEy* **8**, 318 (July 2011).